ACS Medicinal Chemistry Letters

Letter

pubs.acs.org/acsmedchemlett

Development of [^{123}I]IPEB and [^{123}I]IMPEB as SPECT Radioligands for Metabotropic Glutamate Receptor Subtype 5

Kun-Eek Kil, Aijun Zhu, Zhaoda Zhang, Ji-Kyung Choi, Sreekanth Kura, Chunyu Gong, and Anna-Liisa Brownell*

Athinoula A. Martinos Center for Biomedical Imaging, Department of Radiology, Massachusetts General Hospital, Charlestown, Massachusetts 02129, United States

Supporting Information

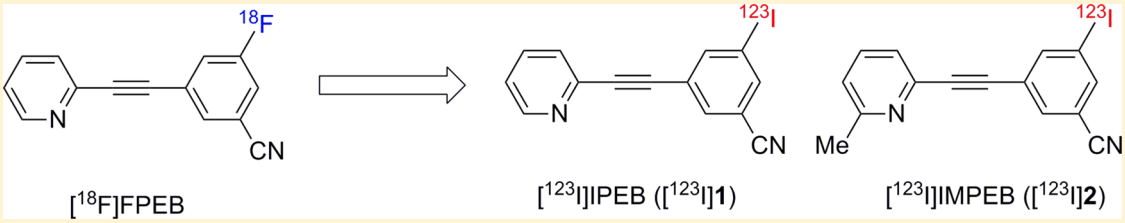

ABSTRACT: $mGlu_5$ play an important role in physiology and pathology to various central nervous system (CNS) diseases. Several positron emission tomography (PET) radiotracers have been developed to explore the role of $mGlu_5$ in brain disorders. However, there are no single photon emission computed tomography (SPECT) radioligands for $mGlu_5$. Here we report development of [^{123}I]IPEB ([^{123}I]**1**) and [^{123}I]IMPEB ([^{123}I]**2**) as $mGlu_5$ radioligands for SPECT. [^{123}I]**1** and [^{123}I]**2** were produced by copper(I) mediated aromatic halide displacement reactions. The SPECT imaging using mouse models demonstrated that [^{123}I]**1** readily entered the brain and accumulated specifically in $mGlu_5$-rich regions of the brain such as striatum and hippocampus. However, in comparison to the corresponding PET tracer [^{18}F]FPEB, [^{123}I]**1** showed faster washout from the brain. The binding ratios of the striatum and the hippocampus compared to the cerebellum for [^{123}I]**1** and [^{18}F]FPEB were similar despite unfavorable pharmacokinetics of [^{123}I]**1**. Further structural optimization of **1** may lead to more viable SPECT radiotracers for the imaging of $mGlu_5$.

KEYWORDS: *metabotropic glutamate receptor subtype 5 ($mGlu_5$), negative allosteric modulator (NAM), single photon emission computed tomography (SPECT), in vivo imaging, [^{123}I]IPEB, [^{123}I]IMPEB*

Glutamate is the most abundant excitatory neurotransmitter in vertebrates, which acts on two main types of membrane receptors: ionotropic glutamate receptors and metabotropic glutamate receptors (mGluRs).[1,2] mGluRs belong to family C of G-protein-coupled receptors (GPCRs).[3] To date, eight mGluR subtypes have been identified that are subdivided into three groups based on sequences, preferred signal transduction mechanisms, and pharmacology.[4] Of eight subtypes of mGluRs, $mGlu_5$ is a member of group I mGluRs along with $mGlu_1$, and it is mainly expressed postsynaptically.[5] In contrast to group II and group III mGluRs, which stimulate inhibitory cyclic adenosine monophosphate pathways via $G_{\alpha i/o}$ subunit of G protein, group I mGluRs interact with $G_{\alpha q}$ subunit of G-protein to stimulate downstream effectors and tyrosine kinases, such as phospholipase C-β, mitogen-activated protein kinase, and phosphoinositide 3 kinase.[5,6] In recent years, negative allosteric modulators (NAMs) of $mGlu_5$ that bind to the transmembrane domains have been developed for their therapeutic potential in a variety of central nervous system (CNS) disorders including pain,[7] Parkinson's disease (PD),[8] drug abuse,[9] fragile X syndrome,[10] epilepsy,[11] and anxiety.[12]

However, positron emission tomography (PET) has played an important role in the development of potential therapeutics for CNS diseases by imaging receptor distribution, concentration, functions in normal and pathological states, and occupancy of potential drug candidate in the brain. Since the first selective $mGlu_5$ antagonist was identified in 1999,[13] a large number of potent, subtype selective, and structurally diverse NAMs have been described.[14] Many $mGlu_5$ PET tracers have been reported, in which 3-[^{18}F]fluoro-5-(pyridin-2-ylethynyl)-benzonitrile ([^{18}F]FPEB),[15,16] [^{11}C]ABP688,[17] and [^{11}C]-SP203[18] have been translated into human studies (Figure 1a).[19−21] We have developed several PET radioligands for $mGlu_5$[16,22] and investigated interplay of glutamatergic and dopaminergic system in rat model of PD by in vivo imaging of modulation of $mGlu_5$ expression and dopamine transporter and D_2 receptor function during degeneration.[23] The PET imaging of $mGlu_5$ showed a relationship between glutamatergic system and neuroinflammation.[24]

In spite of such accomplishments in PET imaging, the effort to develop single photon emission computed tomography (SPECT) radioligands for $mGlu_5$ has been almost negligible.

Received: January 6, 2014
Accepted: April 6, 2014
Published: April 6, 2014

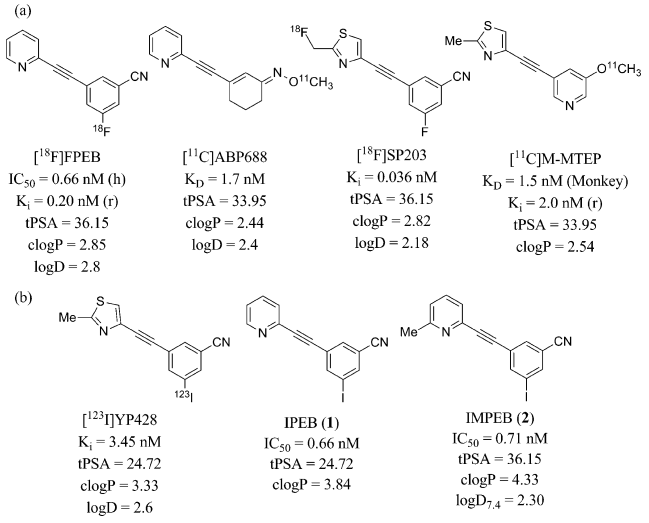

Figure 1. (a) Examples of the published $mGlu_5$ PET ligands.[15−18,29] (b) Molecular properties of SPECT radioligand [^{123}I]YP428, iodo-compounds IPEB (**1**) and IMPEB (**2**).

To date, only one $mGluR_5$ SPECT agent ([^{123}I]YP428; Figure 1b) was reported at the fifth ISR meeting in 2004 for studying cocaine addiction.[25] In comparison to PET radionuclides, SPECT radionuclide such as iodine-123 ($t_{1/2}$ = 13.2 h) has relatively longer half-life and can be bought commercially, thus offering more flexibility in tracer synthesis, lower cost, and better access to the technique.[26,27] Technical advancements in the field have also dramatically improved the spatial resolution for SPECT measurements.[28] Therefore, a reliable SPECT radioligand for $mGlu_5$ would make a big impact on biomedical research of glutamate neurotransmitter and the development of potential therapeutics for CNS diseases.

There are additional challenges for the incorporation of an iodine-123 atom into $mGlu_5$ ligands since it could add significant lipophilicity to the parent molecule, therefore increasing the risk of nonspecific binding. [^{123}I]YP428 can be considered as a derivative of the PET tracer, 3-([^{11}C]methoxy)-5-((2-methyl-1,3-thiazol-4-ylethynyl)pyridine ([^{11}C]M-MTEP) (Figure 1a),[29] in which its methoxy group is replaced by an iodine. Although they have good in vitro properties, both [^{123}I]YP428 and [^{11}C]M-MTEP show fast washout in the brain. Optimal SPECT radioligands should have reasonable slow washout to allow flawless image quality. It is advantageous to design and develop SPECT agents based on promising $mGlu_5$ PET tracers, which have shown not only good in vitro properties but also excellent in vivo results. We and other research groups have demonstrated previously that [^{18}F]FPEB (Figure 1a) is a superior PET tracer for $mGlu_5$.[15,16] It has fast uptake and slow washout in $mGlu_5$ abundant brain regions such as striatum and hippocampus and fast washout in $mGlu_5$ deficient region such as cerebellum. Because [^{18}F]FPEB shows excellent properties as a PET radiotracer, we like to develop the iodine-123 labeled compounds based on the structure of [^{18}F]FPEB. It is also known that the compounds 3-iodo-5-(pyridin-2-ylethynyl)benzonitrile (IPEB (**1**)) and 3-iodo-5-((6-methylpyridin-2-yl)ethynyl)benzonitrile (IMPEB (**2**)) (Figure 1b) have shown good inhibitory activity against $mGlu_5$, in which the IC_{50} are 0.66 and 0.71 nM, respectively.[30] The required affinity for a radiotracer is related to the receptor concentration. It is reported that B_{max} values for $mGlu_5$ are ranging from 21 nM (hypothalamus) to 83 nM (caudate/putamen) in rat.[31] With the criteria of $B_{max}/K_D \gg 1$, a tracer with an affinity <5 nM, and preferably <2 nM, is desired.[15,30] For achieving low nonspecific binding as well as good blood−brain barrier (BBB) penetration, which is often related to lipophilicity, a $logD_{7.4}$ value between 1 and 3 is preferred.[30] Although the cLogP values of **1** and **2** are higher than 3, the experimental value ($logD_{7.4}$ = 2.30) of **2** is well below its calculated value (cLogP = 4.33). Therefore, we anticipate that **1** will exhibit appropriate lipophilicity for brain imaging application since the cLogP (3.84) of **1** is lower than that of **2**. It has also been suggested that compounds with effective BBB penetration preferably have a polar surface area (tPSA) of <60, and molecular weight under 450.[32] Compounds **1** and **2** definitely meet these requirements. Here we report the syntheses and preliminary evaluation of [^{123}I]IPEB ([^{123}I]**1**) and [^{123}I]IMPEB ([^{123}I]**2**) for imaging $mGlu_5$.

Scheme 1 shows the syntheses of nonradioactive reference compounds **1** and **2**, precursors **5a** and **5b**, and radioactive

Scheme 1. Syntheses of Nonradioactive Compounds (1 and 2) and Radioligands ([^{123}I]1 and [^{123}I]2); RCYs Are Decay Corrected

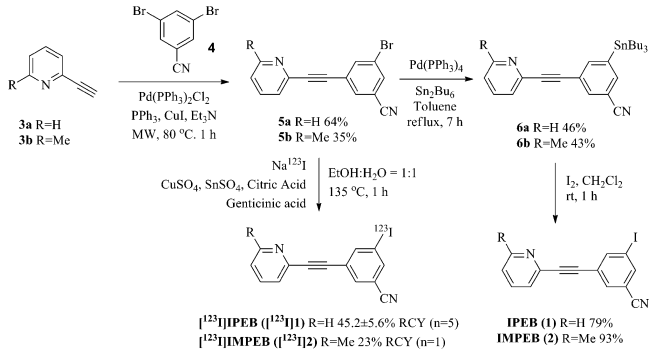

products [^{123}I]**1** and [^{123}I]**2**. Compounds **5a** and **5b** were obtained by Sonogashira coupling reaction between 3,5-dibromobenzonitrile (**4**) and 2-ethynylpyridine derivative (**3a** or **3b**), respectively. The bromo-compounds, **5a** and **5b**, were converted into tributylstannyl derivatives (**6a** and **6b**, respectively) using bis(tributyltin) and tetrakis-(triphenylphosphine)palladium(0). The tributylstannyl groups in **6a** and **6b** were iodinated to give nonradioactive compounds **1** and **2**, respectively. The iodine-123 labeling was first attempted under the oxidative condition mediated by chloramine T using tributylstannyl derivatives **6a** and **6b**, respectively. However, this labeling reaction ended up with predominantly the radioactive side products. Desired radioactive products, [^{123}I]**1** and [^{123}I]**2**, were produced less than 20% radiochemical yield (RCY) (Supporting Information C). On the contrary, in the syntheses of nonradioactive compounds using the similar condition, **1** and **2** were major products, respectively. The radiolabeling reactions were then carried out using the bromo-precursor **5a** or **5b** under the reductive condition mediated by copper(I) catalyst to displace bromine with iodine-123. The reaction produced [^{123}I]**1** and [^{123}I]**2** with 45% and 23% decay-corrected RCY, respectively. The specific activity of [^{123}I]**1** was 182.8 GBq/μmol. Figure 2a,b displays the HPLC profile of radiolabeling reactions of [^{123}I]**1** and [^{123}I]**2**, respectively. As Figure 2a shows, the bromo-precursors **5a** and the radioactive products [^{123}I]**1** were well separated by using HPLC equipped with Zorbax Eclipse XDB-Phenyl semi-

dx.doi.org/10.1021/ml500007z | ACS Med. Chem. Lett. 2014, 5, 652−656

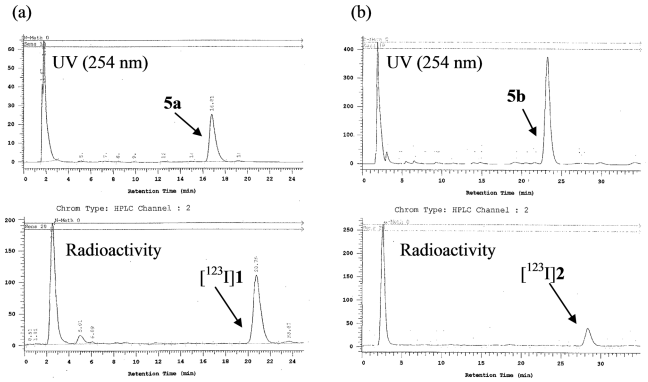

Figure 2. HPLC chromatographs of radiolabeling reactions of (a) [^{123}I]**1** and (b) [^{123}I]**2**.

preparative column (250 × 10 mm, 5 μm, Agilent) eluting with a solution of 0.1 M ammonium formate aqueous solution: CH_3CN (55:45) at a flow rate of 4 mL/min. The similar separation was also achieved between **5b** and [^{123}I]**2** by using Gemini NX-C_{18} semipreparative column (250 × 10 mm, 5 μm, Phenomenex) eluting with a solution of 0.1 M ammonium formate aqueous solution: CH_3CN (45:55) at a flow rate of 4 mL/min (Figure 2b).

After purification, the combined radioactive aliquots were checked for radiochemical purities and coinjected with corresponding nonradioactive standards by using HPLC equipped with Alltima C_{18} analytical column (150 × 4.6 mm, 5 μm, Grace) eluting with a solution of 0.1 M ammonium formate aqueous solution: CH_3CN (40:60 for [^{123}I]**1** and 35:65 for [^{123}I]**2**). Both of the radioactive aliquots display over 98% radiochemical purities, and coinjection of the radioactive aliquots with nonradioactive standard (**1** or **2**) confirmed that the isolated radioactive species are authentic radioactive products (see Supporting Information D).

Because [^{123}I]**1** was obtained in higher yield and may have lower lipophilicity than [^{123}I]**2**, we selected it for preliminary evaluation in mouse studies. Around 11.5−15.5 MBq of [^{123}I]**1** in 10% ethanol saline solution was administered by tail vein injection. The images of mouse brain were acquired by a 4-head SPECT camera (Triumph II, Trifoil Imaging Inc.), in which 90 deg rotation divided to 16 projections with 30 s frame time. Figure 3 illustrates the SPECT images of mouse brain using [^{123}I]**1** and PET images using [^{18}F]FPEB, which show accumulation of [^{123}I]**1** (SPECT study) and [^{18}F]FPEB (PET study) in a mouse brain at the coronal striatal and hippocampal level. Both studies show activity distribution at the time interval 4−20 min after administration of the radioligand in the anesthetized mice. Those images demonstrated that [^{123}I]**1** readily crossed BBB, and its major accumulation was observed in hippocampus and striatum, the regions that were reported to have the most abundant $mGlu_5$ expression along with olfactory bulb, lateral septum, and cortex.[33,34]

Time−activity curves (TACs) of (a) [^{123}I]**1** and (b) [^{18}F]FPEB in a mouse model were generated from SPECT and PET data for striatum, hippocampus, and cerebellum (Figure 4a,b). TACs of [^{123}I]**1** show fast uptake and washout from brain within the first 20 min of SPECT scanning, while the corresponding PET ligand [^{18}F]FPEB has fast uptake but slow washout from striatum and hippocampus and fast washout from cerebellum, which gave consistent results with previous study with rats.[16] Thus, the structural change from fluorine to

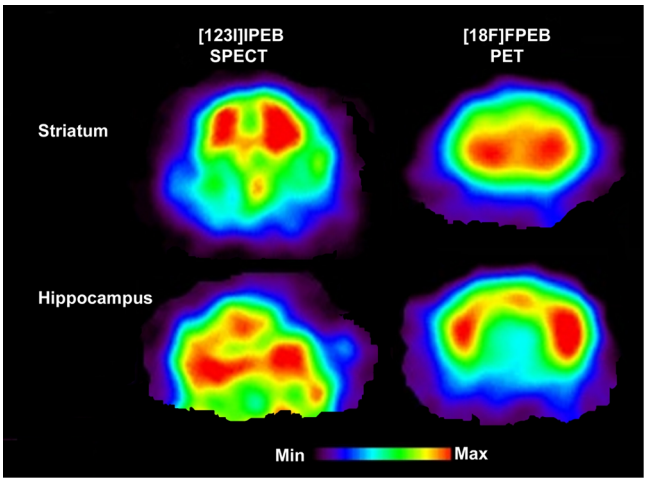

Figure 3. SPECT images with [^{123}I]**1** and PET images with [^{18}F]FPEB show the accumulation of the labeled ligands on striatal and hippocampal level in the mouse brain. The slice thickness in the SPECT images is 0.76 mm, while it is 0.62 mm in PET imaging. The injected radioactivity was 13.5 MBq for SPECT study and 1.5 MBq for PET study demonstrating the significant difference in detection sensitivity between SPECT and PET imaging. The images provide almost equal contrast (target to background ratio).

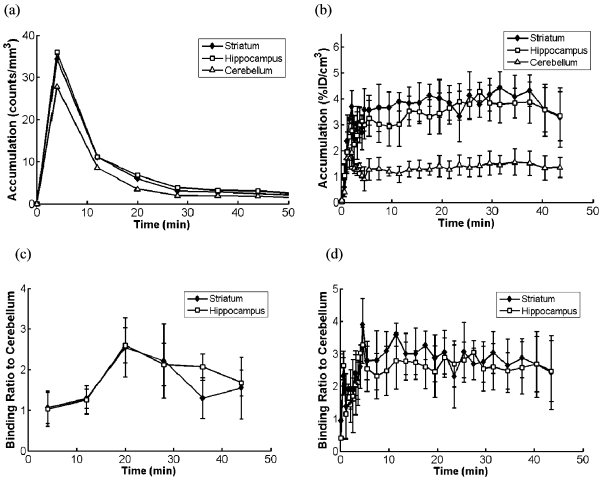

Figure 4. TACs of (a) [^{123}I]**1** and (b) [^{18}F]FPEB in a mouse model show different pharmacokinetics. [^{123}I]**1** has fast washout in all brain areas, while [^{18}F]FPEB is almost in the steady state in striatum and hippocampus having washout from cerebellum. However, the binding ratios to cerebellum of (c) [^{123}I]**1** and (d) [^{18}F]FPEB indicate similar trends for these two PET and SPECT tracers.

iodine induces different pharmacokinetic property, which results in the decreased retention time in the brain. The results indicate that incorporation of iodine-123 impact physicochemical and pharmacological properties, which may include affinity, lipophilicity, and selectivity. First, although IPEB (**1**) has shown good inhibitory activity (IC_{50} = 0.66 nM)[30] against $mGlu_5$, its affinity may not be as good as that of [^{18}F]FPEB (K_i = 0.20 nM)[15] since the IC_{50} value is not always correlated closely to the affinity value.[35] Second, [^{123}I]**1** may have higher lipophilicity than [^{18}F]FPEB, therefore increasing the risk of nonspecific binding. Finally, the selectivity to other receptors such as $mGlu_1$ may be different from [^{18}F]FPEB. These properties will be studied to understand the exact reasons that cause the fast washout of [^{123}I]**1** and to get insight for designing

dx.doi.org/10.1021/ml500007z | ACS Med. Chem. Lett. 2014, 5, 652−656

a suitable SPECT radioligand for $mGlu_5$. However, when TACs of striatum and hippocampus were divided by TACs of cerebellum to derive binding ratio, the graphical trends for [^{123}I]**1** and [^{18}F]FPEB were similar to each other (Figure 4c,d).

Specificity of [^{123}I]**1** was investigated by preinjection of 3-((2-methyl-4-thiazolyl)ethynyl)pyridine hydrochloride (MTEP·HCl) (a NAM of $mGlu_5$; 10 mg/kg i.v. 2 min before radioactivity injection) as a blocking agent for $mGlu_5$. The SPECT images obtained during 24 min after injection of radioactivity were summed, and the images obtained in the baseline study were compared to the data from the blocking study. Blocking with MTEP·HCl reduced accumulation of [^{123}I]**1** by 31% in the whole brain, 34% in the hippocampus, and 42% in the striatum (Figure 5). Thus, this study indicates that [^{123}I]**1** has specific binding to $mGlu_5$.

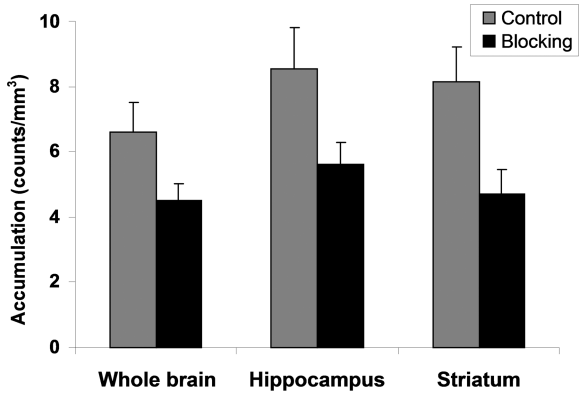

Figure 5. Injection of MTEP·HCl (10 mg/kg i.v. 2 min before radioactivity) reduced accumulation of [^{123}I]**1** by 31% in the whole brain, 34% in the hippocampus, and 42% in the striatum indicating similar specificity as reported previously for [^{18}F]FPEB.[16] Cumulative accumulation is presented at the time interval 0−24 min.

In conclusion, [^{123}I]**1** and [^{123}I]**2** were obtained by copper(I) mediated iodine displacement reaction using corresponding aryl bromide substrates, **5a** and **5b**, respectively. The SPECT imaging using mouse models demonstrated that [^{123}I]**1** readily entered the brain and accumulated specifically in $mGlu_5$-rich regions of the brain such as striatum and hippocampus and that blockade with 10 mg/kg MTEP reduced about 40% of the activity in these regions, thus indicating its specificity to $mGlu_5$. However, in comparison to the corresponding PET tracer [^{18}F]FPEB, [^{123}I]**1** showed the decreased retention time in the brain, which may effect the quality of the imaging. The results also showed that the binding ratio between regions of interest to reference tissue for [^{123}I]**1** and [^{18}F]FPEB were similar despite an unfavorable pharmacokinetic property, the fast washout of [^{123}I]**1**. Further structural optimization based on the IPEB scaffold may lead to the development of more viable SPECT radiotracers for the imaging of $mGlu_5$.

■ ASSOCIATED CONTENT

Supporting Information

Detailed procedure and molecular property of chemistry, radiochemistry, imaging experiments, and supporting data. Spectra of ^{1}H NMR and ^{13}C NMR are also provided. This material is available free of charge via the Internet at http://pubs.acs.org.

■ AUTHOR INFORMATION

Corresponding Author

*(A.-L.B.) E-mail: abrownell@mgh.harvard.edu.

Funding

Funding was provided by NIBIB-R01EB012864 and NIMH-R01MH91684 to A.-L.B. Authors would like to acknowledge supporting grants for the instrumentation 1S10RR029495-01, 1S10RR026666-01, and 1S10RR023452-01.

Notes

The authors declare no competing financial interest.

■ ACKNOWLEDGMENTS

Authors are grateful to Mr. Bryan McIntosh and Ms. Joann Zhang from TriFoil Imaging for the maintenance and operation of Triumph-II PET-SPECT-CT Preclinical Imaging System.

■ ABBREVIATIONS

$mGlu_5$, metabotropic glutamate receptor subtype 5; mGluR, metabotropic glutamate receptor; NAM, negative allosteric modulator; CNS, central nervous system; PD, Parkinson's disease; BBB, blood−brain barrier; SPECT, single photon emission computed tomography; PET, positron emission tomography; [^{18}F]FPEB, 3-[^{18}F]fluoro-5-(pyridin-2-ylethynyl)-benzonitrile; [^{11}C]M-MTEP, 3-([^{11}C]methoxy)-5-((2-methyl-1,3-thiazol-4-ylethynyl)pyridine; [^{123}I]IPEB, 3-[^{123}I]iodo-5-(pyridin-2-ylethynyl)benzonitrile; [^{123}I]IMPEB, 3-[^{123}I]iodo-5-((6-methylpyridin-2-yl)ethynyl)benzonitrile; MTEP·HCl, 3-((2-methyl-4-thiazolyl)ethynyl)pyridine hydrochloride; tPSA, polar surface area; RCY, radiochemical yield; TAC, time−activity curve

■ REFERENCES

(1) Conn, P. J. Physiological roles and therapeutic potential of metabotropic glutamate receptors. *Ann. N.Y. Acad. Sci.* **2003**, *1003*, 12−21.

(2) Watkins, J. C.; Jane, D. E. The glutamate story. *Br. J. Pharmacol.* **2006**, *147*, S100−S108.

(3) Foord, S. M.; Bonner, T. I.; Neubig, R. R.; Rosser, E. M.; Pin, J.-P.; Davenport, A. P.; Spedding, M.; Harmar, A. J. International union of pharmacology. XLVI. G protein-coupled receptor list. *Pharmacol. Rev.* **2005**, *57*, 279−288.

(4) Conn, P. J.; Pin, J.-P. Pharmacology and functions of metabotropic glutamate receptors. *Annu. Rev. Pharmacol. Toxicol.* **1997**, *37*, 205−237.

(5) Niswender, C. M.; Conn, P. J. Metabotropic glutamate receptors: physiology, pharmacology, and disease. *Annu. Rev. Pharmacol. Toxicol.* **2010**, *50*, 295−322.

(6) Francesconi, A.; Duvoisin, R. M. Role of the second and third intracellular loops of metabotropic glutamate receptors in mediating dual signal transduction activation. *J. Biol. Chem.* **1998**, *273*, 5615−5624.

(7) Bleakman, D.; Alt, A.; Nisenbaum, E. S. Glutamate receptors and pain. *Semin. Cell Dev. Biol.* **2006**, *17*, 592−604.

(8) Ossowska, K.; Konieczny, J.; Wardas, J.; Pietraszek, M.; Kuter, K.; Wolfarth, S.; Pilc, A. An influence of ligands of metabotropic glutamate receptor subtypes on parkinsonian-like symptoms and the striatopallidal pathway in rats. *Amino Acids* **2007**, *32*, 179−188.

(9) Carroll, F. I. Antagonists at metabotropic glutamate receptor subtype 5: Structure activity relationships and therapeutic potential for addiction. *Ann. N.Y. Acad. Sci.* **2008**, *1141*, 221−232.

(10) Krueger, D. D.; Bear, M. F. Toward fulfilling the promise of molecular medicine in fragile X syndrome. *Annu. Rev. Med.* **2011**, *62*, 411−429.

(11) Alexander, G. M.; Godwin, D. W. Metabotropic glutamate receptors as a strategic target for the treatment of epilepsy. *Epilepsy Res.* **2006**, *71*, 1−22.
(12) Swanson, C. J.; Bures, M.; Johnson, M. P.; Linden, A.-M.; Monn, J. A.; Schoepp, D. D. Metabotropic glutamate receptors as novel targets for anxiety and stress disorders. *Nat. Rev. Drug Discovery* **2005**, *4*, 131−144.
(13) Varney, M. A.; Cosford, N. D.; Jachec, C.; Rao, S. P.; Sacaan, A.; Lin, F. F.; Bleicher, L.; Santori, E. M.; Flor, P. J.; Allgeier, H.; Gasparini, F.; Kuhn, R.; Hess, S. D.; Velicelebi, G.; Johnson, E. C. SIB-1757 and SIB-1893: selective, noncompetitive antagonists of metabotropic glutamate receptor type 5. *J. Pharmacol. Exp. Ther.* **1999**, *290*, 170−181.
(14) Zhang, Z.; Brownell, A.-L. Imaging of Metabotropic Glutamate Receptors (mGluR)s. In *Neuroimaging: Clinical Applications*; Bright, P., Ed.; InTech, Open Access Publisher: Rijeka, Croatia, 2012; pp 499−532.
(15) Hamill, T.; Krause, S.; Ryan, C.; Bonnefous, C.; Govek, S.; Seiders, T. J.; Cosford, N. D.; Roppe, J.; Kamenecka, T.; Patel, S.; Gibson, R. E.; Sanabria, S.; Riffel, K.; Eng, W.; King, C.; Yang, X.; Green, M. D.; O'Malley, S. S.; Hargreaves, R.; Burns, H. D. Synthesis, characterization, and first successful monkey imaging studies of metabotropic glutamate receptor subtype 5 (mGluR5) PET radiotracers. *Synapse* **2005**, *56*, 205−216.
(16) Wang, J.; Tueckmantel, W.; Zhu, A.; Pellegrino, D.; Brownell, A.-L. Synthesis and preliminary biological evaluation of 3-[^{18}F]fluoro-5-(2-pyridinylethynyl)benzonitrile as a PET radiotracer for imaging metabotropic glutamate receptor subtype 5. *Synapse* **2007**, *61*, 951−961.
(17) Ametamey, S. M.; Kessler, L. J.; Honer, M.; Wyss, M. T.; Buck, A.; Hintermann, S.; Auberson, Y. P.; Gasparini, F.; Schubiger, P. A. Radiosynthesis and preclinical evaluation of ^{11}C-ABP688 as a probe for imaging the metabotropic glutamate receptor subtype 5. *J. Nucl. Med.* **2006**, *47*, 698−705.
(18) Siméon, F.; Brown, A. K.; Zoghbi, S. S.; Patterson, V. M.; Innis, R. B.; Pike, V. W. Synthesis and simple ^{18}F-labeling of 3-fluoro-5-(2-(2-(fluoromethyl)thiazol-4-yl)ethynyl)benzonitrile as a high affinity radioligand for imaging monkey brain metabotropic glutamate subtype-5 receptors with positron emission tomography. *J. Med. Chem.* **2007**, *50*, 3256−3266.
(19) Wong, D. F.; Waterhouse, R.; Kuwabara, H.; Kim, J.; Brasic, J. R.; Chamroonrat, W.; Stabins, M.; Holt, D. P.; Dannals, R. F.; Hamill, T. G.; Mozley, P. D. ^{18}F-FPEB, a PET radiopharmaceutical for quantifying metabotropic glutamate 5 receptors: a first-in-human study of radiochemical safety, biokinetics, and radiation dosimetry. *J. Nucl. Med.* **2013**, *54*, 388−396.
(20) Ametamey, S. M.; Treyer, V.; Streffer, J.; Wyss, M. T.; Schmidt, M.; Blagoev, M.; Hintermann, S.; Auberson, Y.; Gasparini, F.; Fischer, U. C.; Buck, A. Human PET studies of metabotropic glutamate receptor subtype 5 with ^{11}C-ABP688. *J. Nucl. Med.* **2007**, *48*, 247−252.
(21) Kimura, Y.; Simeon, F. G.; Hatazawa, J.; Mozley, P. D.; Pike, V. W.; Innis, R. B.; Fujita, M. Biodistribution and radiation dosimetry of a positron emission tomographic ligand, ^{18}F-SP203, to image metabotropic glutamate subtype 5 receptors in humans. *Eur. J. Nucl. Med. Mol. Imaging* **2010**, *37*, 1943−1949.
(22) Yu, M.; Tueckmantel, W.; Wang, X.; Zhu, A.; Kozikowski, A. P.; Brownell, A.-L. Methoxyphenylethynyl, methoxypyridylethynyl and phenylethynyl derivatives of pyridine: synthesis, radiolabeling and evaluation of new PET ligands for metabotropic glutamate subtype 5 receptors. *Nucl. Med. Biol.* **2005**, *32*, 631−640.
(23) Pellegrino, D.; Cicchetti, F.; Wang, X.; Zhu, A.; Yu, M.; Saint-Pierre, M.; Brownell, A.-L. Modulation of dopaminergic and glutamatergic brain function: PET studies on Parkinsonian rats. *J. Nucl. Med.* **2007**, *48*, 1147−1153.
(24) Drouin-Ouellet, J.; Brownell, A.-L.; Saint-Pierre, M.; Fasano, C.; Emond, V.; Trudeau, L.-E.; Levesque, D.; Cicchetti, F. Neuroinflammation is associated with changes in glial mGluR5 expression and the development of neonatal excitotoxic lesions. *Glia* **2011**, *59*, 188−199.
(25) Alagille, D.; Cosgrove, K.; Baldwin, R.; Amici, L.; Staley, J.; Tamagnan, G. [^{123}I]YP428, first SPECT imaging agent of mGluR5 receptors. *5th International Symposium on Radiohalogens*; Whistler, B.C. Canada, 2004; Abstract no. *CS24*.
(26) Zhang, L.; Villalobos, A. Recent advances in the development of PET and SPECT tracers for brain imaging. *Annu. Rep. Med. Chem.* **2012**, *47*, 105−119.
(27) Pimlott, S. L.; Sutherland, A. Molecular tracers for the PET and SPECT imaging of disease. *Chem. Soc. Rev.* **2011**, *40*, 149−162.
(28) Sharma, S.; Ebadi, M. SPECT neuroimaging in translational research of CNS disorders. *Neurochem. Int.* **2008**, *52*, 352−362.
(29) Krause, S.; Hamill, T. G.; Seiders, T. J.; Ryan, C.; Sanabria, S.; Gibson, R. E.; Patel, S.; Cosford, N. D.; Roppe, J. R.; Hargreaves, R. J.; Burns, H. D. In vivo characterizations of PET ligands for the mGlu5 receptor in rhesus monkey. *Mol. Imaging Biol.* **2003**, *5*, 166.
(30) Alagille, D.; DaCosta, H.; Chen, Y.; Hemstapat, K.; Rodriguez, A.; Baldwin, R. M.; Conn, J. P.; Tamagnan, G. D. Potent mGlu5 antagonists: pyridyl and thiazolyl-ethynyl-3,5-disubstituted-phenyl series. *Bioorg. Med. Chem. Lett.* **2011**, *21*, 3243−3247.
(31) Patel, S.; Ndubizu, O.; Hamill, T.; Chaudhary, A.; Burns, H. D.; Hargreaves, R.; Gibson, R. E. Screening cascade and development of potential positron emission tomography radiotracers for mGluR5: in vitro and in vivo characterization. *Mol. Imaging Biol.* **2005**, *7*, 314−323.
(32) Hitchcock, S. A.; Pennington, L. D. Structure−brain exposure relationships. *J. Med. Chem.* **2006**, *49*, 7559−7583.
(33) Romano, C.; Sesma, M. A.; McDonald, C. T.; O'Malley, K.; Van den Pol, A. N.; Olney, J. W. Distribution of metabotropic glutamate receptor mGluR5 immunoreactivity in rat brain. *J. Comp. Neurol.* **1995**, *355*, 455−469.
(34) Abe, T.; Sugihara, H.; Nawa, H.; Shigemoto, R.; Mizuno, N.; Nakanishi, S. Molecular characterization of a novel metabotropic glutamate receptor mGluR5 coupled to inositol phosphate/Ca^{2+} signal transduction. *J. Biol. Chem.* **1992**, *267*, 13361−13368.
(35) Kenakin, T.; Onaran, O. The ligand paradox between affinity and efficacy: can you be there and not make a difference? *Trends Pharmacol. Sci.* **2002**, *23*, 275−280.